Comparison of ECMWF Cloud Cover with Radar Derived Values

Robin J. Hogan*, **Christian Jakob**† **and Anthony J. Illingworth**

Department of Meteorology, University of Reading, UK
†European Centre for Medium-Range Weather Forecasts, Reading, UK
***Email: R.J.Hogan@reading.ac.uk.**

INTRODUCTION

The limited spatial resolution available to global atmospheric models means that in addition to the usual prognostic variable of cloud water content, it is necessary for them to include some estimate of the sub-gridscale fluctuation in cloudiness. Most models diagnose cloud cover every timestep from prognostic model variables such as humidity and cloud water content, but in the current version of the European Centre for Medium-Range Weather Forecasts (ECMWF) model, cloud cover is itself formulated as a prognostic variable (Tiedtke 1993). The physical basis underlying the treatment of this parameter (as either diagnostic or prognostic) is somewhat uncertain, and consequently errors in model radiative fluxes are often blamed on poor model cloud cover. The fundamental role played by clouds in the earth's radiation budget means that it is important that this parameter can be predicted accurately for climate simulations to be reliable.

A previous attempt to validate the cloud cover in the ECMWF model used AVHRR data to estimate the total cloud cover for a model gridbox through the whole depth of the atmosphere (Karlsson 1996), but there is clearly a need for vertically-resolved observations of to be used to perform the validation at each model level. In this study, ECMWF cloud cover is compared with that derived by three active instruments located at Chilbolton, England, for a three-month period. Throughout most of the depth of the atmosphere one of two vertically-pointing cloud radars (the 'Rabelais' operating at 35 GHz and the 'Galileo' operating at 94 GHz) is used, but up to the freezing level we use the cloud base reported by a lidar ceilometer in preference, since this instrument is more effective at detecting liquid water clouds. However, it is rapidly attenuated so cannot be used above the base of the first cloud.

An earlier comparison by Mace et al. (1998) employed a much simpler technique; each model gridbox was determined to be either cloudy or cloud-free according to whether a 35 GHz radar observed any cloud in it during the model timestep, and this was compared with the same 'binary' information derived from the ECMWF cloud fields.

METHOD

The principle of the technique is quite straightforward; daily time-height sections of radar reflectivity are divided into boxes centred on the model height levels and timesteps, and cloud cover is then simply taken to be the fraction of radar pixels in each box that register the presence of cloud. The model has 31 levels in the vertical and a timestep of 20 minutes. The radar data have been averaged over 2 minutes and 150 metres, which increases the sensitivity by 7 dB over the raw 10 second/75 metre data, yet still provides several tens of pixels in each box from which cloud cover can be calculated. The horizontal resolution of the model is around 60 km, so there is a question as to whether measurements taken at a single site during a 20 minute period can be representative of all the clouds in an area this size; the wind speed would have to be 50 m s^{-1} for clouds to be sampled from both sides of the gridbox.

Care has been taken to ensure that only signals from clouds are included in the analysis. The main consequence is that the radar returns below around 500 m cannot be used because of leakage by the transmit pulse into the receiver and the presence

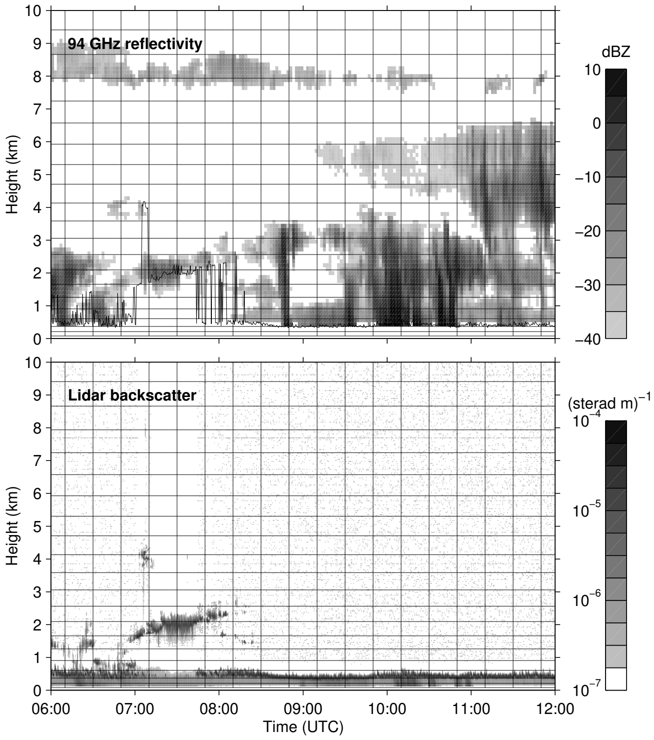

Fig. 1: An example of the data from which cloud cover can be derived, taken on Christmas Day 1998. The top panel shows radar reflectivity measured at 94 GHz, with lidar-derived cloud base indicated by the solid line. The bottom panel depicts lidar backscatter coefficient. Overlayed on each are the model gridboxes.

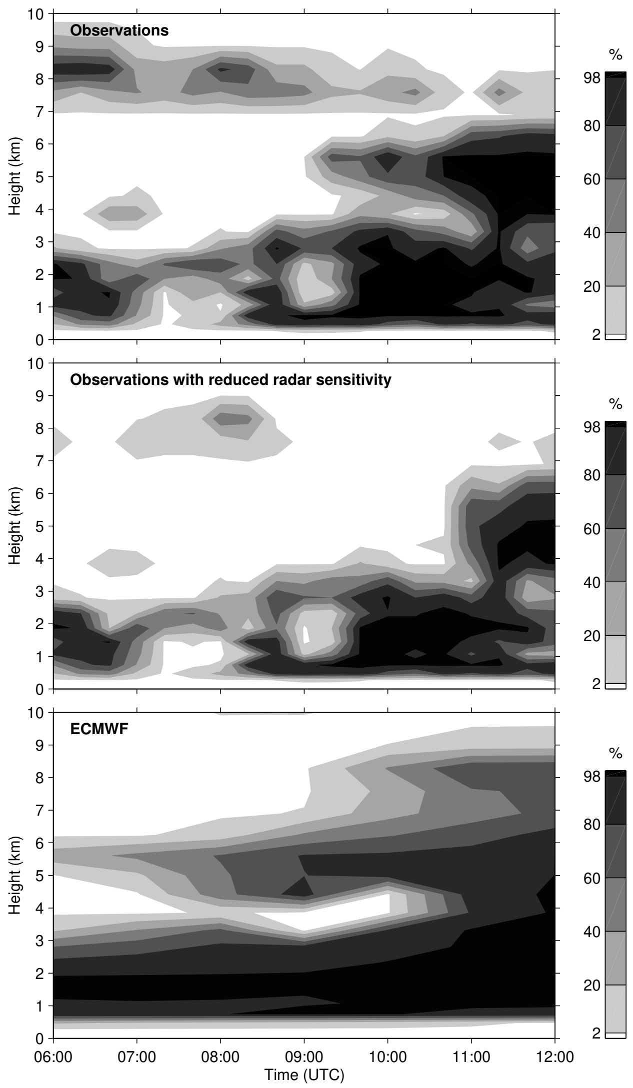

Fig. 2: The top panel shows cloud cover derived from the observations presented in Fig. 1, and the second lower panel shows cloud cover derived in the same way but after reducing the radar sensitivity by 10 dB. The lower panel depicts the corresponding values predicted by the ECMWF model.

of ground clutter. The common problem of insects in the boundary layer is non-existent at 51°N during winter, when the data for this study were taken. A further difficulty, however, is that in the presence of rain the radar is unable detect cloud base. We therefore use cloud base measured by a Vaisala CT75K lidar ceilometer operating at 905 nm (30 second, 30 metre resolution) to estimate cloud cover at the base of clouds warmer than 0°C, where the temperature is taken from the model. It is found that even stratocumulus can have sufficient drizzle falling out of it that cloud base height according to the radar can be underestimated by several hundred metres. Invariably the signal from the lidar is rapidly extinguished in liquid water clouds and the radar must be used above.

To illustrate the retrieval process, Fig. 1 shows 6 hours of lidar and 94 GHz radar data taken on 25 December 1998. Except for the period between 07:00 and 08:00 UTC, the lidar signal is completely blocked by low-level cloud, which has a base at 400 m. Note that the lidar also detects aerosols in the boundary layer, although they give a much lower return. The model gridboxes are shown superimposed. The cloud cover derived from these observations is shown in the top panel of Fig. 2. The 0°C isotherm was at around 2.3 km on this day.

It is naturally very important the instruments are able to detect the large majority of all clouds. Liquid water clouds tend to have very distinct boundaries in the short wave and there is therefore no difficulty in detecting them with the lidar. Cirrus clouds on the other hand do not have distinct boundaries and there is always some doubt as to whether the radar is detecting their full extent. The 94 GHz radar in this example had a minimum detectable reflectivity of -55 dBZ at 1 km and -35 dBZ at 10 km. It was shown by Brown et al. (1995) that virtually all 'radiatively significant' cirrus has a reflectivity at 94 GHz of greater than -30 dBZ. However we can illustrate the potential problem by reducing the sensitivity of the radar by 10 dB at all heights. The cloud cover derived after degrading the data in this way is shown in the second panel of Fig. 2. Clearly much less cirrus is observed but it is interesting to note that the retrieved cloud cover at low levels is virtually unchanged, although this is mainly because the radar is intrinsically much more sensitive to nearby clouds. It is worth mentioning that attenuation by rain can attenuate the (two-way) signal at 94 GHz by up to around 10 dB, and the light rain at 08:50 and between 10:00 and 11:00 UTC may have caused a certain amount of attenuation of the signal and reduced the amount of cirrus detected. This is much less of a problem at 35 GHz.

ECMWF cloud cover for this period is shown in the lower panel of Fig. 2; note that although the model timestep is 20 minutes, only the hourly fields are recorded routinely. The model predicted a similar amount of cloud between 0.5 and 3 km as was observed, although its cloud-cover field is much smoother. There are significant differences between the predicted and observed amounts of mid-level and high cloud.

RESULTS

Cloud cover has been calculated from the near-continuous observations taken between 24 October 1998 and 23 January 1999 at Chilbolton, and Fig. 3 shows a comparison of observed and modelled cloud cover during a six-week period in November/December 1998. It is apparent from the fluctuations in the observed cloud cover in Fig. 2 that 20 minutes is not really long enough for adequate sampling of the cloud in a model gridbox, so the observations have been averaged over an hour. The larger scale features appear to match up reasonably well, but an objective comparison is required to highlight where the model is deficient.

The first step in such an analysis is to compare the distribution of cloud cover for the entire three month period. The first panel of Fig. 4 shows mean cloud cover as a function of height from the model and the observations, and the following two show this information split up into 'frequency of occurrence' and 'amount when present', using a trigger level of 5%. Figure 4 also shows the frequency distribution of cloud

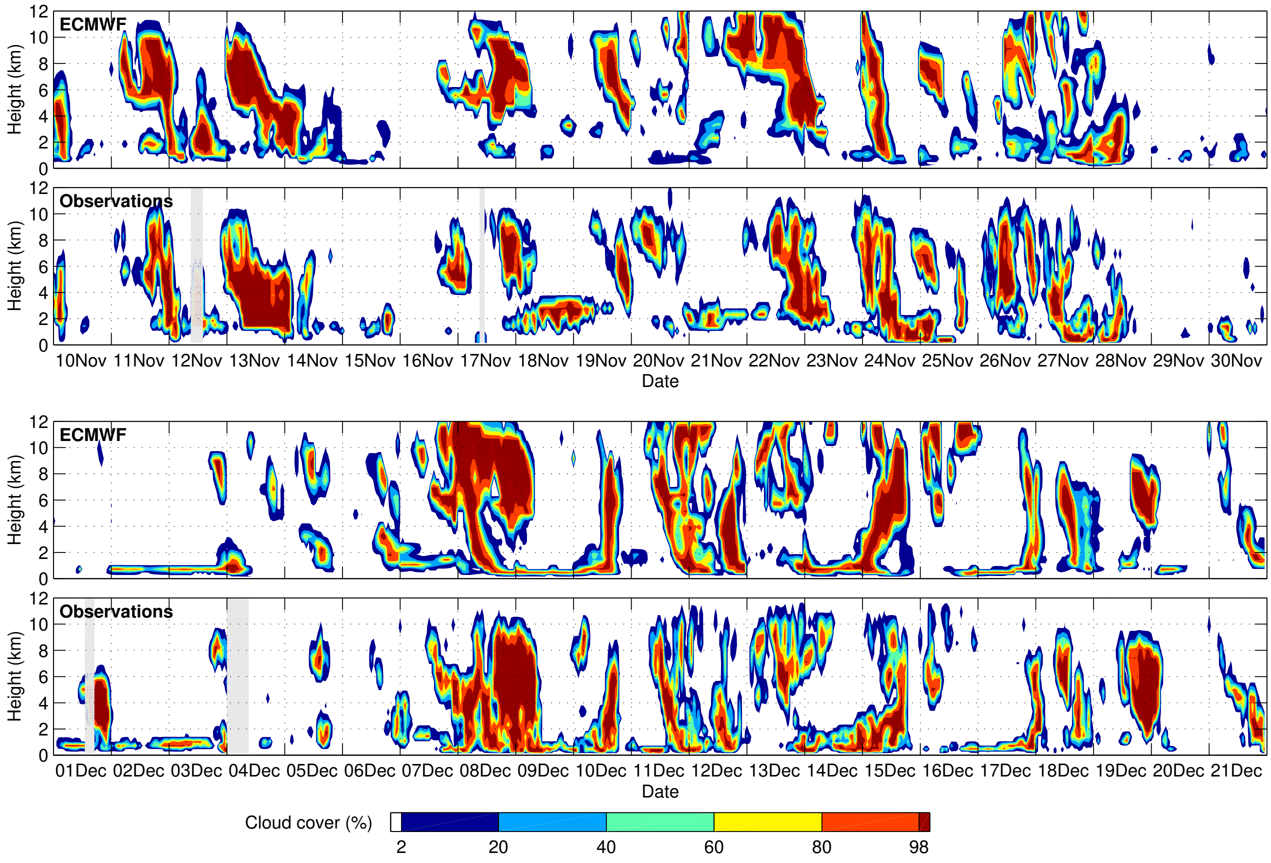

Fig. 3: Comparison of observed and ECMWF model cloud cover at Chilbolton for a six-week period. Only the 94 GHz radar was used during this time. The very light grey rectangles indicate when the radar was not operating vertically.

cover at the three different height levels. We see that on average the model tends to predict too little low and medium-level cloud but too much high cloud. However, it performs much better in simulating the frequency of cloud occurrence (analogous to the comparison performed by Mace et al. 1998). Hence the problem is not of clouds being produced when there are none (or vice versa) but of simulating the right cloud cover when clouds are present.

One problem with the comparison is that the observations cannot distinguish between ice cloud and ice precipitation (i.e. snow) whereas the model treats them separately such that snow does not contribute to cloud cover. In reality of course they are a continuum, but this ambiguity results in the tendency, apparent from Fig. 4, that a little more cloud is observed at altitudes of around 4 km than is modelled.

The difference between the model and the observations at high levels is much greater, with the model apparently overestimating cloud cover considerably. There is obviously the possibility that there are tenuous cirrus cloud tops not detected by the radar, and as already mentioned, attenuation by rain and low-level liquid water cloud can considerably reduce the sensitivity of the 94 GHz radar to cirrus.

The next step is to see how well the model agrees with the observations on a pixel-by-pixel basis. The first panel of Fig. 5 shows the correlation coefficient of the two fields versus height and lag time. Throughout most of the troposphere the correlation is around 0.5 and there is no lag, but we find the surprising result that in the lowest 1 km the model tends to simulate cloud features up to 3 hours before they are observed.

The second panel of Fig. 5 shows the mean absolute difference in percentage cloud cover between the the model and the observations as a function of height. Throughout most of the depth of the atmosphere the difference is around 18% (expressed in percent because that is the unit of cloud cover, i.e. this figure does not mean that the mean absolute difference is 18% of the mean). From Fig. 4 we see that this is not much less than the typical mean cloud covers of between 15% and 30%, implying that the model is performing poorly. However, the requirement that the model should be accurate to one hour and one model level is perhaps overly stringent, and it is certainly not essential for radiation that the model is this accurate. It would be fairer to first average both fields onto a coarser grid that better reflects the spatial and temporal accuracy required.

Mean absolute difference is shown as a function of time of day in the third panel of Fig. 5, and we see that the error increases from 15% at the beginning of the day to around 18% at

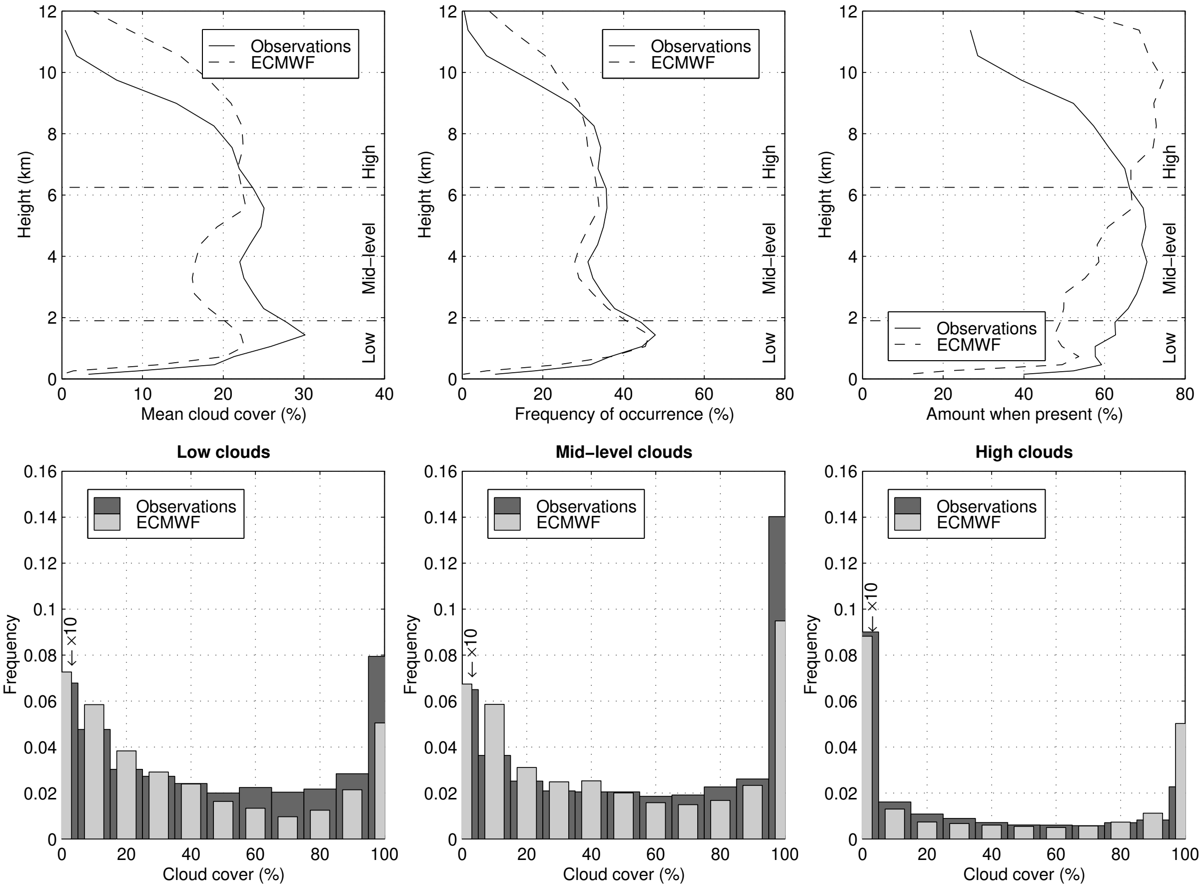

Fig. 4: Cloud cover statistics for the entire three-month period. The top row panels depict (as a function of height) mean cloud cover, frequency that cloud cover is over 5% and mean cloud cover when more than 5%. The bottom row shows the frequency distribution of cloud cover in the three height bands used by the model (bounded by the 800 mb and 450 mb surfaces). Note that the bars centred on 0% are shown at one tenth of their true value.

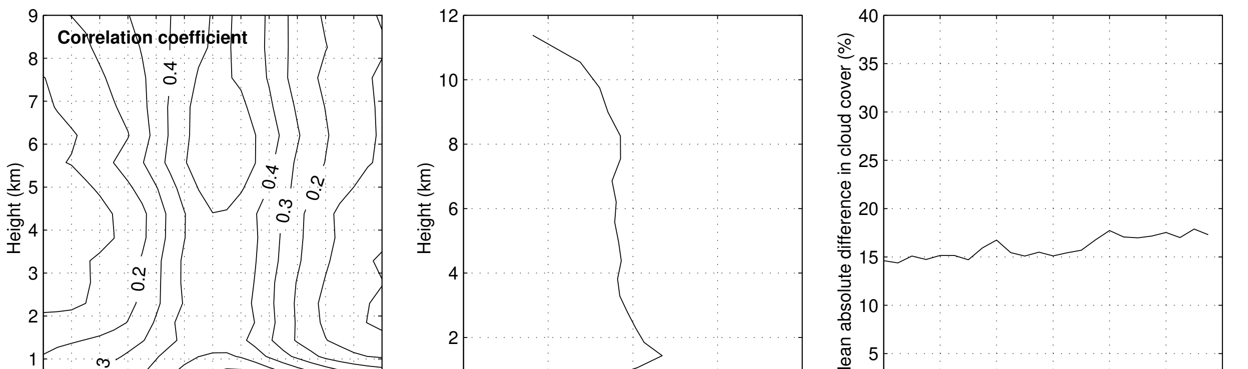

Fig. 5: The first panel shows the correlation of the observed and modelled cloud cover fields as a function of height and lag time. A positive lag corresponds to the model simulating features before they are observed. The second and third panels show the mean absolute difference between the two fields versus height and time of day respectively.

the end. This is simply because the model fields were produced on a daily basis from forecasts initialised at 12 UTC the previous day, and the accuracy of the model naturally decreases with time. This also explains the sharp changes often seen in model cloud cover between 23 UTC and 00 UTC the following day.

CONCLUSIONS AND FUTURE WORK

It has been shown that the very different but complimentary scattering properties of radar and lidar have the capability to perform a very valuable role in validating the representation of clouds in models. From a climatology point of view the model is found to be reasonably good at forecasting the frequency that cloud cover is more than 5%, but when cloud is present it performs poorly in predicting the actual cloud cover. On a pixel-by-pixel basis the model performance is also poor, but a fairer test needs to be devised involving appropriate filtering of the data.

A number of improvements could be made to the algorithm that derives cloud cover from the raw observations. The model consistently generates more high-level cloud than is measured, but the sensitivity of the radar at this altitude is a problem when there is attenuation. Throughout the three-month period a drop-counting rain gauge was deployed at Chilbolton, and visual inspection of the radar data suggests that extinction of the signal at 94 GHz is only a problem in moderate to heavy rain. A suitable rain-rate threshold could be chosen in order to reject from the comparison any cloud cover derived when attenuation is likely to be very strong.

The distinction between cloud and precipitation has been very successful in the case of rain, with the lidar ceilometer always able to locate cloud base when the radar signal is dominated by the contribution from the much-larger raindrops. In ice-phase precipitation such a distinction is not really possible and snow is therefore included in the observed cloud cover fields. Hence it would be appropriate to use the snow flux held in the model to estimate ‘snow cover’, which could be combined with model cloud cover before performing the comparison with observations.

We also intend to compare ice water content derived from reflectivity and temperature (Liu and Illingworth 1997) or from dual-wavelength radar (Hogan et al. 1999) with the values held in the model. This study also highlights the possibility that active instruments could provide real-time information on clouds for assimilation into models; the proposed spaceborne cloud radar would be particularly suited to this task.

ACKNOWLEDGEMENTS

We wish to thank the Radiocommunications Research Agency at the Rutherford Appleton Laboratory for the use of the radars and lidar at Chilbolton. The Galileo radar was developed for the European Space Agency by Officine Galileo, the Rutherford Appleton Laboratory and the University of Reading, under ESTEC Contract No. 10568/NL/NB. The Rabelais radar is on loan from the University of Toulouse. This research received funding from NERC (grant GR3/8765).

REFERENCES

Brown, P. R. A., A. J. Illingworth, A. J. Heymsfield, G. M. McFarquhar, K. A. Browning and M. Gosset, 1995: The role of spaceborne millimeter-wave radar in the global monitoring of ice-cloud. *J. Appl. Met.,* **34**(11), 2346–2366.

Hogan, R. J., A. J. Illingworth and H. Sauvageot, 1999: Measuring crystal size in cirrus using 35 and 94 GHz radars. *J. Atmos. Oceanic Tech.*, in press.

Karlsson, K. G., 1996: Validation of modelled cloudiness using satellite-estimated cloud climatologies. *Tellus A,* **48**(5), 767–785.

Liu, C. and A. J. Illingworth, 1997: Cirrus cloud ice water content retrieval algorithms for a future spaceborne cloud radar. *Proc. 28th AMS Conference on Radar Meteorology,* Austin, Texas. 109–110.

Mace, G. G., C. Jakob and K. P. Moran, 1998: Validation of hydrometeor occurrence predicted by the ECMWF using millimeter wave radar data. *Geophys. Res. Let.,* **25**(10), 1645–1648.

Tiedtke, M., 1993: Representation of clouds in large-scale models. *Mon. Weath. Rev.,* **121**, 3040–3061.